ACS Biomaterials SCIENCE & ENGINEERING

pubs.acs.org/journal/abseba

Article

Hydroxyapatite Pellets as Versatile Model Surfaces for Systematic Adhesion Studies on Enamel: A Force Spectroscopy Case Study

Johannes Mischo, Thomas Faidt, Ryan B. McMillan, Johanna Dudek, Gubesh Gunaratnam, Pardis Bayenat, Anne Holtsch, Christian Spengler, Frank Müller, Hendrik Hähl, Markus Bischoff, Matthias Hannig, and Karin Jacobs*

Cite This: *ACS Biomater. Sci. Eng.* 2022, 8, 1476–1485

Read Online

ACCESS | Metrics & More | Article Recommendations | Supporting Information

ABSTRACT: Research into materials for medical application draws inspiration from naturally occurring or synthesized surfaces, just like many other research directions. For medical application of materials, particular attention has to be paid to biocompatibility, osseointegration, and bacterial adhesion behavior. To understand their properties and behavior, experimental studies with natural materials such as teeth are strongly required. The results, however, may be highly case-dependent because natural surfaces have the disadvantage of being subject to wide variations, for instance in their chemical composition, structure, morphology, roughness, and porosity. A synthetic surface which mimics enamel in its performance with respect to bacterial adhesion and biocompatibility would, therefore, facilitate systematic studies much better. In this study, we discuss the possibility of using hydroxyapatite (HAp) pellets to simulate the surfaces of teeth and show the possibility and limitations of using a model surface. We performed single-cell force spectroscopy with single *Staphylococcus aureus* cells to measure adhesion-related parameters such as adhesion force and rupture length of cell wall proteins binding to HAp and enamel. We also examine the influence of blood plasma and saliva on the adhesion properties of *S. aureus*. The results of these measurements are matched to water wettability, elemental composition of the samples, and the change in the macromolecules adsorbed over time on the surface. We found that the adhesion properties of *S. aureus* were similar on HAp and enamel samples under all conditions: Significant decreases in adhesion strength were found equally in the presence of saliva or blood plasma on both surfaces. We therefore conclude that HAp pellets are a good alternative for natural dental material. This is especially true when slight variations in the physicochemical properties of the natural materials may affect the experimental series.

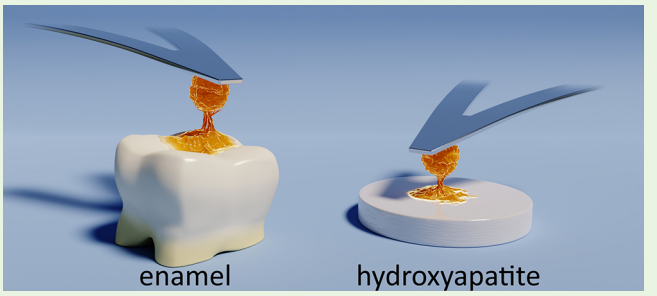

KEYWORDS: *Staphylococcus aureus, adhesion, saliva, blood plasma, hydroxyapatite, enamel, single-cell force spectroscopy, AFM, contact angle, ellipsometry*

INTRODUCTION

The mineral part of human enamel as well as of bones is, apart from small, varying amounts of carbonate, magnesium, and trace elements such as fluorine, mainly composed of hydroxyapatite (HAp, $Ca_{10}(PO_4)_6(OH)_2$).[1−3] Research into HAp as a biomaterial, its synthesis, application development, and improvements has progressed over the last decades: for instance, HAp-based cements are readily available for use, robust HAp compounds with high fracture toughness and wear resistance have been developed, and porous HAp scaffolds for bone regeneration have been proposed.[1,4,5] In most modern medical applications, bone and teeth are still most often mended with implant materials, such as titanium in artificial hip joints or screws.[6,7] Such procedures are often associated with severe medical complications such as prosthetic implant failures or aseptic loosening.[8−12] For dental implants for instance, a 2015 study of over 1000 dental implants shows that up to 10% of patients receiving dental implants suffer from postoperative infections, two-thirds of which must have their implant removed.[13] Bacterial biofilm formation at the interface between biological tissues and implants is a common cause of inflammation, so its prevention is essential.[14] Bacterial infections start with the adhesion of single, planktonic bacteria to a surface. The bacteria then start to grow into microorganism consortia, embedded in an extracellular matrix in which the bacteria are protected from host defense mechanisms and antibacterial therapy.[15,16] A common approach is to prevent or hinder the bacterial adhesion process as the first step of bacterial biofilm

Received: July 19, 2021
Accepted: February 22, 2022
Published: March 9, 2022

formation.[17] Research into bacterial biofilm formation is, however, in most cases either carried out on highly artificial laboratory surfaces, such as silicon wafers or glass slides, or on natural samples, that are subject to severe sample-to-sample changes due to external factors like age, material composition, and morphology.[18−21] We propose systematic studies of factors influencing biofilm formation, using surfaces that offer both the verisimilitude of a material used in practice and the advantages of reproducibility and well-defined material properties, such as surface topography.

In this study, we focus on the natural material of enamel as a case study and HAp as a basis for further systematic research. HAp is known to meet the requirements of closeness to enamel and mimics both the biocompatibility and characteristics concerning bacterial biofilms of the natural material.[22−25] We compare surface properties of artificially synthesized HAp pellets to natural bovine enamel, investigate single-bacterium adhesion, and determine the underlying adhesion forces and ruptures lengths.

Single-cell force spectroscopy (SCFS) with an atomic force microscope has proven to be an ideal method to determine the adhesion parameters of bacterial cell wall macromolecules forming interactions with the surface.[26−28] For the purpose of this study, we have chosen the opportunistic pathogen *Staphylococcus aureus*, as it forms clinically relevant biofilms[29] and is a common cause of implant failures and inflammation in the oral cavity[30−32] and beyond.[12]

It is known that the surface chemistry, hydrophobicity, and surface charge[33,34] or adsorbates deposited on top of a surface influence the bacterial adhesion process. Such adsorbates could be ions, molecules, proteins,[35,36] or other macromolecules contained in bodily fluids in contact with the surface, such as salivary macromolecules[19,39,40] or blood plasma.[37,38] For the purpose of this study, we therefore use well-characterized samples and also examine the influence of conditioning films consisting exclusively of the macromolecules present in either saliva or blood plasma because any material in the body is inevitably in contact with host fluids. For example, it has been shown that a salivary macromolecule film, termed pellicle, forms within seconds after a surface is brought into contact with saliva.[41] The pellicle reaches a thickness of around 7 nm within 3 min and is free from bacteria at this early stage.[42,43] We also expose bacteria to saliva to mimic the natural case, in which a bacterium comes into contact with the surfaces we chose from the oral cavity setting.

We report a direct measure of the reduction of bacterial adhesion strength in the presence of biomolecules of bodily fluids. Further, we evaluate whether HAp pellets, as well-characterized, artificially synthesized surfaces, can mimic enamel in its performance with respect to bacterial adhesion and biocompatibility. While such a synthetic surface would be an excellent basis for further systematic studies on parameters influencing these properties, it also offers the opportunity to replace an animal donor and to reduce the variances between individual experimental setups currently based on teeth of different origin.

MATERIALS AND METHODS

Bacteria and Bacterial Probes. For each experiment, *Staphylococcus aureus* strain SA113 was freshly cultured as follows: The bacteria were inoculated and grown from a deep-frozen glycerol stock on Tryptic Soy Agar Plates with 5% sheep blood (Becton Dickinson, Heidelberg, Germany) at 37 °C for 24 h. A discrete colony was resuspended in Tryptic Soy Broth (TSB, Becton Dickinson) at a culture to flask volume of 1:10 and cultivated at 37 °C and 150 rpm for 16 h. To obtain cells from the exponential growth phase, the bacterial solution was diluted by 1:100 in fresh TSB and incubated for another 2.5 h at the same settings, resulting in a bacterial solution with an Optical Density at 600 nm (OD 600) of 0.5. We removed the debris and extracellular material by washing with 1 mL of bacterial solution three times using 1 mL of phosphate buffered saline (PBS, pH 7.4, Carl Roth GmbH, Karlsruhe, Germany) as the replacement supernatant after centrifuging at 20 000 m/s^2. The bacterial solution was set to an OD 600 of 0.1. Before each AFM tip functionalization, the bacteria were vortexed to disrupt bacterial aggregates and subsequently diluted 1:100 in PBS. A drop of the diluted bacterial solution was spotted in a Petri dish, and a single bacterium was then attached to a calibrated tipless AFM cantilever (MLCT-O10 E, Bruker-Nano, Santa Barbara, US-CA) via dopamine using the technique described by Thewes et al.[44] This functionalization was controlled optically with an inverted microscope before and after the measurement.

Human Samples. The saliva was donated by five volunteers, both male and female, over 18 years of age, with good oral health. Human blood plasma (BP) was obtained from male healthy volunteers older than 18 years. All subjects gave their informed written consent to participate in this study. Pellicle collection and blood plasma protocols were approved by the medical ethic committee of the Medical Association of Saarland, Germany (code numbers 39/20 and 238/03 2016).

Saliva samples were obtained 1.5 h after tooth brushing with toothpaste (dentalux COMPLEX3 Mint Fresh, DENTAL-Kosmetik GmbH, Dresden, Germany). In between, the donors brushed their teeth once without toothpaste 1 h after first brushing and refrained from eating and drinking (except for still water) for the whole time. The saliva obtained was centrifuged at room temperature at 25 000 m/s^2 for 10 min in Falcon tubes (Corning Inc., Corning, US-NY). The supernatant was then transferred to fresh tubes, and the process was repeated once. The remaining saliva from all five participants was mixed, aliquoted, and stored at −20 °C.

The Human BP was derived from freshly drawn blood and centrifuged at 6 000 m/s^2 in S-Monovette lithium-heparin blood collection tubes (Sarstedt, Nümbrecht, Germany) for 2 min. The plasma was transferred to a fresh reaction tube and centrifuged one more time under the same conditions to remove any remaining cell material. The blood plasma was stored in a fresh reaction tube at −80 °C until usage.

Sample Preparation. The hydroxyapatite (HAp) samples were made from compressed and sintered HAp powder (Sigma-Aldrich, Steinheim, Germany) according to the protocol described by Zeitz and Faidt et al.[45] Before usage, the HAp samples were polished, using abrasive paper (SiC, Struers, Willich, Germany) with decreasing coarseness and polishing solution (MSY 0-0.03, Microdiamant, Lengwil, Switzerland: 30 nm diamond particle solution). The debris from polishing was removed by etching in a sodium acetate buffer (pH 4.5) for 7 s and subsequent sonication in ultrapure water (TKA-GenPure, Thermo Fischer Scientific, Waltham, US-MA). The HAp samples used have the same crystal structure, chemical composition, and surface roughness as specified by Zeitz and Faidt et al.[45]

Throughout this study, three pieces of enamel cut from the vestibular surface of three bovine incisor teeth from different animals were used. Bovine dental hard substance has been an established substitute for healthy human teeth in dental studies for many decades.[46−49] Similar to the HAp sample, the enamel was polished in several steps before usage except for the polishing solution, where a suspension of 40 nm sized colloidal silica particles (OP-S, Struers, Ballerup, Denmark, rebranded: now OP-U) was used. Residues were removed in an ethanol ultrasonic bath. All three enamel samples were prepared in the same way.

The generation of homogeneous conditioning films on both HAp and enamel was carried out following these procedures: For a BP coating, the whole sample surface was covered with BP liquid, and it was incubated for 30 min at 37 °C. For salivary pellicle formation, saliva was applied onto the surfaces and incubated for 3 min at room temperature.[42] For both coatings, the surfaces were washed with PBS

https://doi.org/10.1021/acsbiomaterials.1c00925
ACS Biomater. Sci. Eng. 2022, 8, 1476−1485

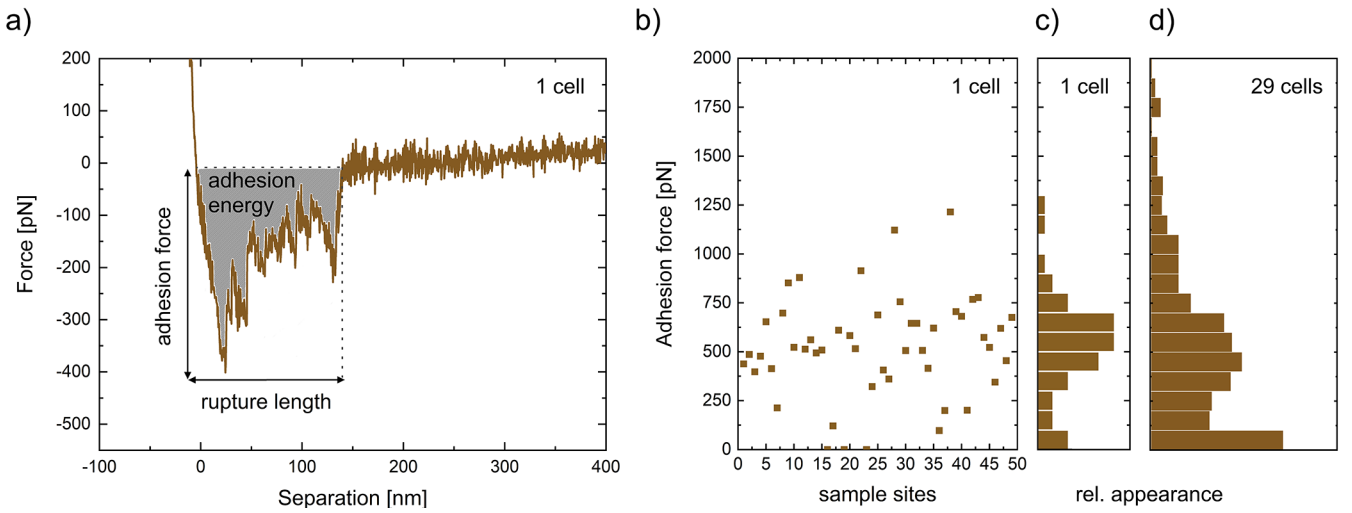

Figure 1. Force distance curves and extracted data: a) exemplary force distance curve of a single *S. aureus* cell on uncoated HAp; b) adhesion force of one and the same cell on 49 different sample sites, c) the respective distribution shown as a histogram, and d) results of force distance curves of all 29 *S. aureus* cells measured under this conditioning combination.

and thereafter kept in fresh PBS. Bacteria, which were exposed to saliva before measurement, were exposed in their immobilized state on the tip of a cantilever for 3 min in 25 μL of saliva at room temperature, and the whole cantilever was washed afterward in PBS.[40]

Sample Characterization. Surface topography of all samples used was acquired by atomic force microscopy (FastScan Bio, Bruker-Nano, Santa Barbara, US-CA). The instrument was operated with Olympus OMCL-AC160TS probes (Tokyo, Japan) in tapping mode. Roughness values were calculated from 30 3D scans of 1 μm × 1 μm (512 × 512 pixels) regions per surface captured at a scan rate of 0.1 Hz and averaged. The number of scans distributed across the samples reveals differences in roughness if present. Tilt and scan line height jumps were removed (routines "PlaneFit 1st order and "Flatten 0th order") using the Nanoscope Analysis 1.9 (Bruker Nano, Santa Barbara, US-CA) software (for exemplary images see SI Figure S1).

The wettability of all surfaces was evaluated by water contact angles in fresh ultrapure water using the sessile drop setting on an OCA 25 instrument (Dataphysics, Filderstadt, Germany). To maintain a wet environment for the coated surfaces, all samples were measured in a water bath with air bubbles pressed onto them to determine advancing and receding contact angles. The air bubbles used were around 500 μm in diameter and were displaced by several millimeters to obtain advancing and receding contact angles.

X-ray photoelectron spectroscopy (XPS) was performed with nonmonochromatized Al−K α excitation ($\hbar\omega$ = 1486.6 eV) using an ESCALAB MKII spectrometer (Vacuum Generators, Hastings, UK, base pressure approximately 10^{-10} mbar). The spectra were normalized by the photoemission cross sections, as proposed by Yeh and Lindau and adjusted with a Shirley background.[50,51]

To determine the molecular weight of the macromolecules of the conditioning films, we performed sodium dodecyl sulfate polyacrylamide gel electrophoresis (SDS-PAGE) and Coomassie-staining as previously described by Trautmann et al.[43] at two different ages of the films. The specimens consisting exclusively of enamel with a total surface area of 8 cm^2 were purified with 3% NaOCl, washed with water, ultrasonicated in 70% isopropyl alcohol, and air-dried before exposure to either saliva or PBS for 3 min at room temperature. Nonadsorbed material was removed with 20 mL of ultrapure water from a pressure cylinder (Buerkle GmbH, Bad Bellingen, Germany). Then, the samples were either directly treated with elution buffer to elute the adsorbed macromolecules or incubated in PBS at room temperature, and the elution was performed 3.5 h later. The elution, subsequent precipitation, and final preparation for SDS-PAGE and Coomassie-staining were conducted.[43]

Single-Cell Force Spectroscopy. With the bacterial probes described above, force−distance measurements on all surfaces were performed with a Bioscope Catalyst AFM (Bruker-Nano, Santa Barbara, US-CA). The force trigger was set to 300 pN, and the lateral distance between two force−distance measurement points was set to 1 μm. The contact time of the bacterium and the surfaces was tested at both the minimal possible time of a few milliseconds[52] (called 0 s surface delay) and 5 s surface delay, during which the force trigger was kept constant. For 0 s surface delay measurements, the loading rate was set to 800 nm/s. To reduce piezo creep, the approach rate was reduced to 100 nm/s on 5 s surface delay measurements.

For the purpose of this study, we focus on the data with 5 s surface delay and attach measurements with 0 s delay in the Supporting Information (SI Figure S2). We measured single bacteria on different hydrophilic surfaces. Using one cell, 49 force−distance curves were recorded at different locations within a rectangular array of 7 μm × 7 μm with 1 μm distances between the locations on each of the three sample surfaces. One bacterium was measured first on one sample (e.g., HAp), then on the respective other sample (e.g., enamel), and again on the first sample to ensure that no significant changes in the force curves such as decreasing adhesion force were observable. Cantilever and bacterium constantly remain in liquid during the measurement. Both samples are within the same Petri dish under the same buffer solution. The sample preconditioning on both surfaces was the same (e.g., untreated) for a single bacterium. The order in which these samples were tested has been randomized from bacterium to bacterium to minimize systematic error. The measurements on the samples were repeated with on average 16 bacteria for each preconditioning combination. From each force−distance curve, it is possible to obtain values for adhesion force (see Figure 1a,b), rupture length, and adhesion energy (see the SI).[34,53] The resulting data histograms (see Figure 1c) of all the cells measured under the same preconditioning were combined into one histogram (see Figure 1d). The resulting histograms discussed in this study give an averaged distribution describing the probability for diverse bacteria. They provide the basis for predictions on adhesion force, energy, or rupture length for further cells to be probed on our surfaces.[54]

Statistical Analysis. Statistical analysis of all data distributions under all coating conditions was conducted, using the Kolmogorov−Smirnov test for normality, the Wilcoxon Signed Rank, and the Kruskal−Wallis test implemented in the OriginPro2021b software (OriginLab, Northampton, US-MA). As the data under consideration (adhesion force, adhesion energy, and rupture length) cannot take values below zero, it cannot be considered normally distributed by mathematical definition. This is also shown by the Kolmogorov−

https://doi.org/10.1021/acsbiomaterials.1c00925
ACS Biomater. Sci. Eng. 2022, 8, 1476−1485

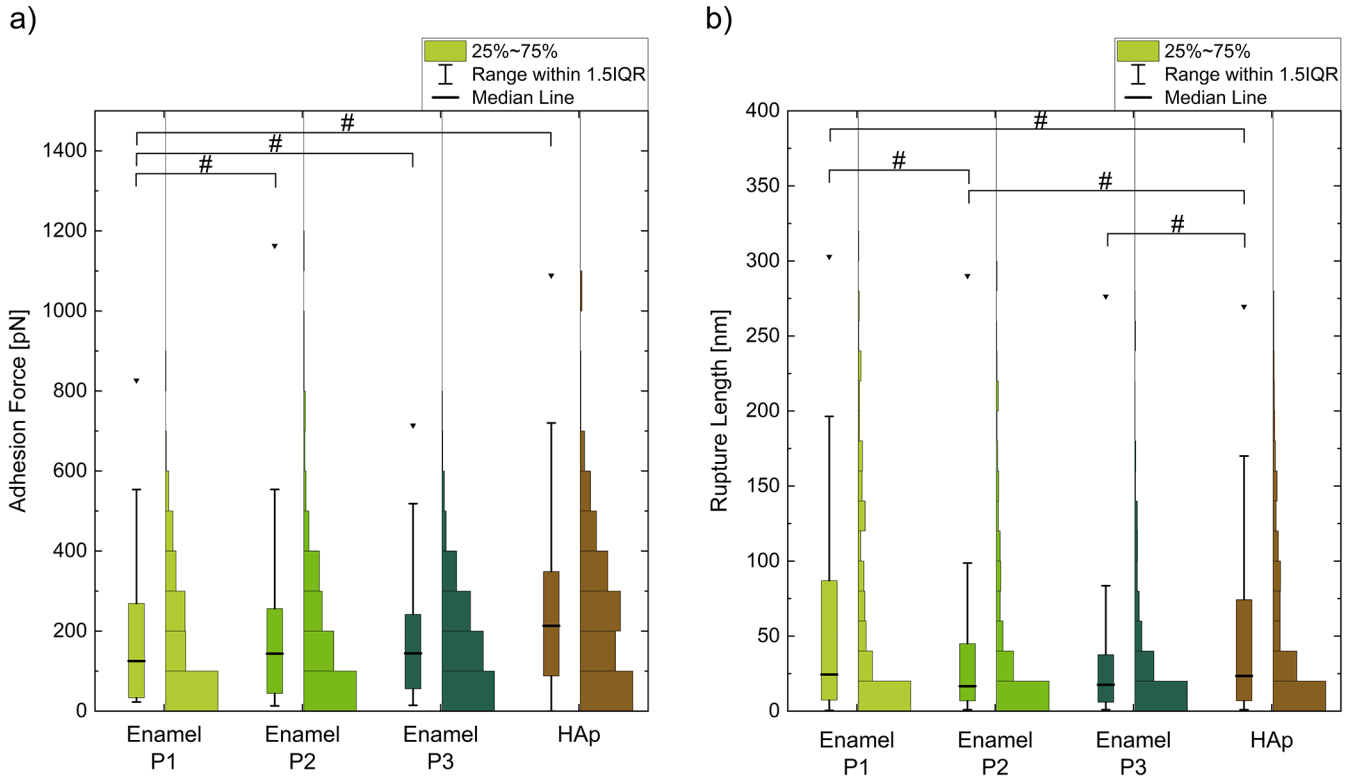

Figure 2. Single-cell force spectroscopy results of eight *S. aureus* cells on three distinct, untreated pieces of enamel and HAp. a) Adhesion forces and b) rupture lengths. The median value (including all values) is given by a black horizontal line. The boxplot's box covers 50% of all data points, and the whiskers give the 1.5 interquartile range (IQR). The black triangles represent the maximum values measured. The level of significance is given by hash signs.

Smirnov test. Due to our experimental layout, we have paired data sets for measurements conducted with the same bacterium. These duplet data sets were tested for significance with the Wilcoxon Signed Rank test. Where the respective significance level of 0.05 has been reached, indication is provided via a hash symbol in the graphs (see Figure 2). To compare the data sets that were not measured with the same bacterium and are therefore uncoupled (e.g., untreated bacterium no. 1 on untreated HAP vs untreated bacterium no. 2 on saliva-incubated HAp), we applied a Kruskal–Wallis test including Dunn's posthoc test. The Dunn's test has been evaluated with Pearson's correlation coefficient and classified after Cohen.[55] The significance levels obtained are presented above the measurement data by asterisks in increasing levels of significance: "*": $r > .10$; "**": $r > .30$; "***": $r > .50$ (highest significance). For reasons of clarity, correlations that were not significantly different were not labeled.

RESULTS AND DISCUSSION

Differences in Enamel. Bovine enamel as a natural material underlies external parameters that cannot be influenced by an experimental setup, such as origin, chemical composition, and porosity of the samples. To evaluate the difference of bacterial adhesion force, energy, and rupture length on different pieces of enamel from different cows, three enamel samples were tested against HAp pellets. The adhesion force and energy distributions of the three enamel surfaces (P1, P2, and P3) are not distinguishable by the Wilcoxon Signed Rank test (see Figure 2, SI Figure 3). Small differences can be seen in the rupture length. Hence, we only analyzed one of the three samples in detail and used it for evaluating different conditioning factors. It is not unreasonable to assume that the cattle from which the samples originate have an influence on the measurement. The bovine tooth samples used were obtained from one slaughterhouse, and the cattle therefore come only from a restricted region in the southwest of Germany. Fluoride content in and on teeth, for instance, is one of the differences found between individual specimens and is widely researched.[56−58] Studies show that fluoride content influences the adhesion of bacteria.[59,60] This will result in teeth samples from cattle of different (global) origin to vary due to differences in fluoride content in drinking water. HAp as a synthetic material has the advantage that it features reproducible chemical composition and roughness. Furthermore, it allows for systematic changes in chemical and mechanical parameters and replaces an animal donor.

Changes in the Conditioning Film. Single-cell force spectroscopy measurements are performed over hours, during which the adsorbed conditioning films are kept in a buffer solution. To monitor the changes such biological surface coatings undergo during our measurement time, we looked at changes in the composition of macromolecules on the surfaces. Our SDS-PAGE eluates of saliva and BP conditioning films show that the molecular weight of macromolecules adsorbed on the surface does not change markedly between start of the experiments and after 3.5 h in PBS (see SI Figure S4). No distinct statement of the amount of macromolecules adsorbed can be reached as small differences in color depth in the lanes could also be attributed to slight variations of the staining agents. Even if we consider the small decrease in color depth as a reduction of adsorbed macromolecules, no correlations between adhesion force and adsorbed amount or rupture length and adsorbed amount were found. This is probably due to the fact that variations in adhesion forces and rupture lengths are quite large between individual bacteria, depending on the study design.[17,40,61,49] The data shows that small changes in the

https://doi.org/10.1021/acsbiomaterials.1c00925
ACS Biomater. Sci. Eng. 2022, 8, 1476−1485

thickness of the film do not influence the adhesion process significantly.

Sample Characterization. XPS reveals that HAp and enamel are very similar in chemical composition, except that HAp does not contain any magnesium, sodium, or fluorine (see SI Figure S5). The root-mean-square roughness (RMS) obtained by AFM of the hydroxyapatite pellet is 0.4(2) nm, and for the enamel sample, it is 1.6(3) nm. Hence, the surfaces feature low, mirror-like surface roughness, and since all 30 scans per sample reveal similar results, seen in the low standard deviation, the surface roughness can be assumed to be homogeneous. In the literature, increased surface roughness has been found both to increase and decrease adhesion.[33,63−66] In a previous study, we revealed that roughness on the nanoscale (RMS ≤ 7 nm) had no influence on adhesion of *S. aureus*.[66] Based on this result, all surfaces used in this study were polished to be smoother than RMS = 7 nm to eliminate the influence of roughness on adhesion measurements.

Our samples are, however, not free of imperfections on a millimeter-scale such as deeper grooves from coarser polishing steps or natural crystal boundaries or cracks in the material. These have no influence on SCFS, as they are negligible due to statistical variation of the cantilever position on the surface (49 positions were probed with each bacterium). Furthermore, the small contact area of *S. aureus* (150 to 350 nm radius)[67] makes incidental measurements in such spots even less probable.

The imperfections of the surfaces, however, have an influence on the contact angle measurement in the form of pinning and a resulting contact angle hysteresis.[68,69] In this study, regions with extreme pinning have been omitted during measurement. Optical contact angle measurement is a macroscopic technique: it provides a mean surface characteristic (on at least a mm scale). To determine the optical contact angle on the samples with and without conditioning films, air bubbles in aqueous surroundings were used. Due to the high hydrophilicity of the samples, contact angles of water droplets in air were too small to be determined (see Table 1).

Table 1. Advancing Water Contact Angle (Adv. CA) and the Contact Angle Hysteresis on All Surfaces with and without Different Conditioning Films Used, Averaged over Three Independent Measurements

	no conditioning film		salivary conditioning film		BP conditioning film	
	HAp	enamel	HAp	enamel	HAp	enamel
Adv. CA [deg]	**26.5**	**22.3**	**18.7**	**22.3**	**12.2**	**16.0**
SD	1.9	2.3	3.5	2.0	3.5	4.2
hysteresis [deg]	**10.3**	**0.3**	**0.8**	**0.9**	**0.3**	**1.4**
error	3.1	3.4	4.5	2.7	4.7	6.0

[The optical contact angle only serves as a qualitative characterization of the surface in this study. In the literature, hydrophobicity is shown to greatly influence the adhesion of bacteria to a surface in both ways, but in general, most bacterial species adhere better to hydrophobic surfaces.[31,34,66,70−72] Comparing an optically determined contact angle of real, imperfect samples with single-cell force spectroscopy data is, however, not advisible as the measurands are acquired on different dimensions: The attractive potential a bacterium faces during adhesion at the nanoscale is typically not the same as the macroscopic attractive potential characterized by an optical contact angle measurement on the millimeter scale.[69] We therefore give no correlation between the contact angle and SCFS adhesion force.]

Adhesion Force and Rupture Length. Overall, 146 individual bacteria have been tested in five different combinations of bodily fluid exposure of both the surface and the bacterium (see Figure 3a). The number of measurements per surface and condition is almost evenly distributed, as individual bacterial cells under the same conditions show larger variations in their adhesion behavior on hydrophilic surfaces.[34,61,62] In Figure 3, each combination is represented by a separate column containing the data in the form of a boxplot and a histogram next to it. For the adhesion measurements, we have chosen data binning in 100 pN steps for the adhesion force measurements and 20 nm steps for the rupture length measurements. The adhesion energy data is provided in the Supporting Information (see SI Figure S6). In the lowest bin, the majority of data captured is close to or not distinguishable from the instrument's noise, and therefore, the lowest bin of the adhesion force is considered as no adhesion for the purpose of this study. To quantify this, the percentage of measurements below 100 pN is indicated next to the lowest bin (see Figure 3a). The correlations between the protein combinations from the Kruskal−Wallis test are given above the data in asterisks. The correlations given are calculated excluding the lowest bin (0−100 pN).

The 0−100 pN bin has great importance in the data evaluation: In a previous study, we could show that on hydrophobic surfaces the adhesion force is highly cell specific, which means that the adhesion force is very reproducible for an individual cell but varies more between different cells.[34] In contrast, the adhesion force is highly stochastic on hydrophilic surfaces, i.e., it varies as much between repetitive measurements of a single cell as between different cells.[34] The rupture lengths, which give the approximate length of the last desorbing molecule, however, vary on both hydrophobic and hydrophilic surfaces from repetition to repetition with the same cell and show a very similar order of magnitude. This led to the conclusion that *S. aureus* adhere to hydrophilic surfaces via few but strongly binding macromolecules.[34,73] To bind (and unbind), the macromolecules need to overcome a potential barrier.[74,75] This is a time-dependent statistical process, so in each of the 49 curves of a single bacterium, a different fraction of macromolecules tethers, resulting in different maximum adhesion forces, rupture lengths, and adhesion energies measured. The percentage of data points in the 0−100 pN bin gives a relative estimate of the height of the potential barrier and is therefore used as one criterium to compare bacterial adhesion under varying conditioning combinations. We exclude this bin from the correlation calculations to compare distributions of adhering macromolecules whose difference or similarity is not visible to the eye. The distribution in the adhesion force graph (see Figure 3a) shows the strongest binding macromolecules of each bacterium, while the adhesion energy (see SI Figure S6) also includes all weaker binding molecules. The median value, calculated based on all data points of each preconditioning, is used as a third parameter to compare different conditioning sets.

Throughout all measurements on both surfaces, the highest median adhesion force is generally found on uncoated surfaces with untreated bacteria (see Figure 3). Thus, any of the bodily fluid combinations tested in this study render the adhesion of a bacterium less likely than the uncoated state. The rupture length is generally lowest for the combination of uncoated bacteria and surfaces, because only the adhesive macromolecules of the bacterium itself are involved (see Figure 3b). The rupture length

https://doi.org/10.1021/acsbiomaterials.1c00925
ACS Biomater. Sci. Eng. 2022, 8, 1476−1485

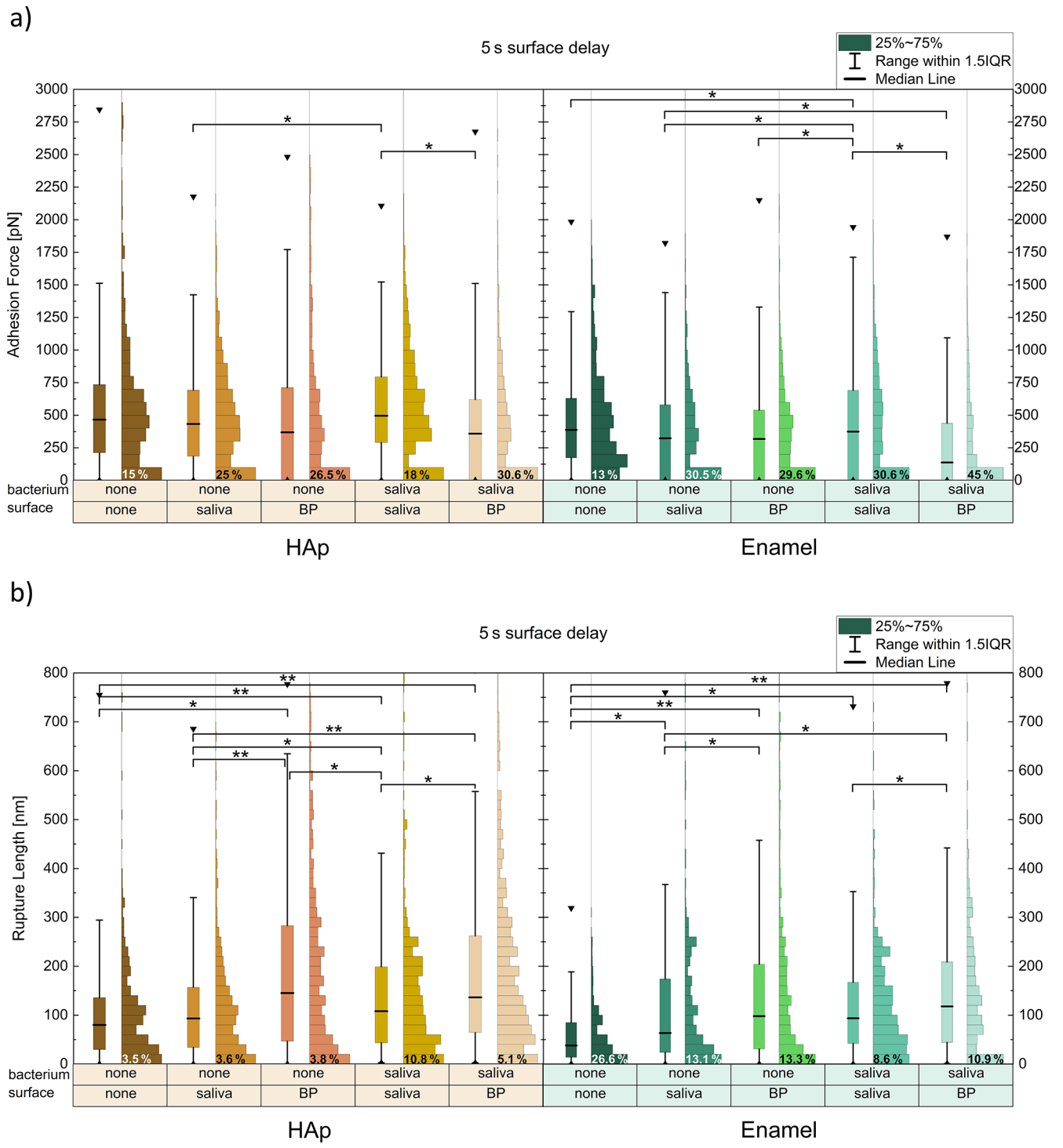

Figure 3. Single-cell force spectroscopy results of 146 *S. aureus* cells on HAp and enamel under all tested conditions in the experimental setup. The conditions are given by a column in the table below a diagram, denoting if and how bacterium and surface were pretreated, w/o saliva or human blood plasma (BP). a) Adhesion forces and b) rupture lengths collected from 16 to 20 bacteria per column with 49 force−distance curves each. The median value (including all values) is given by a black horizontal line. The boxplot's box covers 50% of all data points, and the whiskers give the 1.5 interquartile range (IQR). The black triangles represent the maximum values measured.

of combinations where BP macromolecules were involved are highest, and the saliva-coated surfaces (with and without saliva-treated bacteria) place in between. It is possible that additional hydrogen and ionic bonds can be established on a conditioning film formed on the substratum surface.[76] Whether these are formed or are stronger than the binding of the conditioning film to the surface depends on the bacterial species, the binding partners involved, and the subsurface.[4,31,40,77] For instance, we observe higher rupture length for BP coatings on the surface but no increase in adhesion force compared to the uncoated state and therefore also an increase in adhesion energy (see SI Figure 6). We cannot be certain whether we stretch a weak binding or

https://doi.org/10.1021/acsbiomaterials.1c00925
ACS Biomater. Sci. Eng. 2022, 8, 1476−1485

detach macromolecules from the conditioning films on the surface. If we assume that we detach macromolecules and the binding is so strong that these macromolecules remain bound to the bacterium, we should see a change in adhesion forces between the first force−distance curves and the last ones of each bacterium. We have, however, no indication that the bacteria picked up or detached any macromolecules from the conditioning films which influence the adhesion force, as the first force−distance curve of all bacteria observed can never be considered discordant (see the explanation to Figure 1).

Saliva-treated *S. aureus* on BP-coated surfaces displayed the lowest median adhesion forces in this study. For this condition, the number of observations within the <100 pN bin was highest among all combinations (see Figure 3a), and the incidence without any adhesion was at least twice as high as those recorded for the uncoated states on each surface, making this the bodily fluid combination with the lowest chance of bacteria adhering at all. Yet, if the adhering macromolecules overcome the potential barrier and bind, the same maximum adhesion force distribution values can be reached in comparison to the completely untreated or the BP conditioned surface state. The median adhesion force decreases between unconditioned bacteria and surface and salivary conditioned bacterium on the BP-treated surface by 23% (HAp) and 35% (enamel) (see Figure 3a). For practical applications, this finding suggests that HAp-based material covered by BP is likely to reduce the adhesion of planktonic *S. aureus* cells originating from the oral environment and that overall a lower force is needed to detach them from the surface.

When the same bodily liquid (in this case saliva exposure of bacterium and surface) was used, median adhesion forces on both enamel and HAp were in the same range compared to the uncoated state. Different bodily liquids (saliva on bacterium and BP-coating on surface), however, clearly decreased the maximum adhesion forces observed between bacterial cell and substratum. Furthermore, the percentage of adhesion force values below 100 pN is higher on different bodily liquids than on the same ones, which is again higher than on the unconditioned state. As the blood plasma-coated surfaces were less attractive for saliva-treated bacteria than the saliva-treated surfaces, we conclude that a BP conditioning film is more effective in preventing colonization by *S. aureus* than the formation of the physiological salivary pellicle. Similar findings of reduced adhesion of the same and other bacteria, such as oral bacteria, on surfaces such as glass, polystyrene, elastane, and polyurethane covered with BP macromolecules further support our proposition.[19,38,78,79]

In the case of untreated bacteria, it did not matter for the adhesion force distributions measured whether enamel and HAp were coated with saliva or BP. Even though the rupture lengths varied, the adhesion force distributions were indistinguishable between the two bodily fluid-treated surfaces (see Figure 3a). The percentage of forces measured below 100 pN was also almost identical on each surface and more than 10% higher than the value for the uncoated surfaces. The resulting overall decreases in median adhesion force were 7 to 21% from uncoated to conditioned surfaces, while the median value of BP is always lower of saliva.

Notably, for all combinations of bodily fluids, *S. aureus* cells adhered weaker on enamel than on HAp, although both surfaces exhibited a comparable roughness and similar advancing water contact angles and consist mainly (97%) of the same chemical component.[45] Overall, fewer high force and high rupture length values were measured on enamel compared to HAp under all tested combinations (see Figure 3a, SI Figure 7). On coated surfaces with different bacterial conditionings, also the percentage of low adhesion force values (below 100 pN) was always higher on enamel than on HAp. This leads to a 14 (none-BP) to 61% (saliva-BP) decrease in median adhesion force values. These findings demonstrate that adhesion studies conducted with HAp may not necessarily mirror the adhesion force values that might be seen with the same bacterium on natural enamel. However, the influence of the conditioning films on each surface is remarkably similar. HAp samples therefore still have their value as a substitute for natural enamel in dental research, as they provide a reproducible and consistent surface chemistry, which allows controlled alterations in roughness or fluoride content.[45,80,81] The development of natural enamel, in contrast, is a highly complex process, which is among others influenced by the individual organic content of enamel and external factors,[82] which may lead to larger variations. The nonhydroxyapatite parts of enamel, the ionic substitutes in the mineral component, and/or the crystal orientation, however, seem to make the difference in reaching the lowest force values measured in this study. The exact causes for this are a subject for further investigations.

CONCLUSION

With this study, we propose to utilize the advantages of reproducibility and well-defined material properties found in artificially produced surfaces which mimic natural surfaces. Standardized and well-characterized surfaces like the presented HAp pellets are an essential prerequisite for systematic experimental research on factors influencing bacterial adhesion. Results on, for example, antibacterial coatings or reagents obtained with such samples are thus easily comparable. A quantitative correlation to natural samples can be established by a few measurements on single, well-characterized teeth samples. Performing the same experiments instead only on natural material requires a complete and sometimes very complex characterization for each sample with respect to, for example, roughness, chemical composition of the surface and the material below, crystal domain properties, and porosity.

HAp pellets provide a reproducible and consistent surface chemistry, which allows controlled alterations such as in roughness or fluoride content. Overall, the differences observed between HAp and bovine enamel in our study are comparably small. In the present study, bodily fluids were used to coat the surfaces, while the adhesion force of *S. aureus* was measured on coated and uncoated surfaces of both types. The coatings reduce the adhesion forces of *S. aureus* significantly, thus, they prevent the adhesion of planktonic *S. aureus* cells coming from the oral cavity as well as facilitate their removal by providing the lowest forces required for detachment. Thereby, the coating with blood plasma performed best on the artificial and on the natural surfaces. These results demonstrate that for studies like the present one, hydroxyapatite pellets are a valuable surrogate for natural enamel in dental research.

ASSOCIATED CONTENT

Supporting Information

The Supporting Information is available free of charge at https://pubs.acs.org/doi/10.1021/acsbiomaterials.1c00925.

Surface topology of enamel and HAp; 0 s surface delay AFM data; adhesion energy AFM data HAp vs enamel; SDS-PAGE data of saliva and BP over time; XPS data of

https://doi.org/10.1021/acsbiomaterials.1c00925
ACS Biomater. Sci. Eng. 2022, 8, 1476−1485

enamel and HAp; adhesion energy AFM data of different conditioned surfaces; and Wilcoxon test (PDF)

AUTHOR INFORMATION

Corresponding Author

Karin Jacobs − *Experimental Physics and Center for Biophysics, Saarland University, 66123 Saarbrücken, Germany; Max Planck School Matter to Life, 69120 Heidelberg, Germany*; Email: k.jacobs@physik.uni-saarland.de

Authors

Johannes Mischo − *Experimental Physics and Center for Biophysics, Saarland University, 66123 Saarbrücken, Germany*; orcid.org/0000-0002-9668-6603

Thomas Faidt − *Experimental Physics and Center for Biophysics, Saarland University, 66123 Saarbrücken, Germany*; orcid.org/0000-0003-2035-786X

Ryan B. McMillan − *Experimental Physics and Center for Biophysics, Saarland University, 66123 Saarbrücken, Germany*; Present Address: Harvard University, MA, USA

Johanna Dudek − *Clinic of Operative Dentistry, Periodontology and Preventive Dentistry, Saarland University, 66421 Homburg/Saar, Germany*

Gubesh Gunaratnam − *Institute of Medical Microbiology and Hygiene and Center for Biophysics, Saarland University, 66421 Homburg/Saar, Germany*

Pardis Bayenat − *Experimental Physics and Center for Biophysics, Saarland University, 66123 Saarbrücken, Germany*

Anne Holtsch − *Experimental Physics and Center for Biophysics, Saarland University, 66123 Saarbrücken, Germany*; orcid.org/0000-0003-2454-593X

Christian Spengler − *Experimental Physics and Center for Biophysics, Saarland University, 66123 Saarbrücken, Germany*; orcid.org/0000-0002-0504-1149

Frank Müller − *Experimental Physics and Center for Biophysics, Saarland University, 66123 Saarbrücken, Germany*; orcid.org/0000-0001-8955-5317

Hendrik Hähl − *Experimental Physics and Center for Biophysics, Saarland University, 66123 Saarbrücken, Germany*; orcid.org/0000-0002-2708-0990

Markus Bischoff − *Institute of Medical Microbiology and Hygiene and Center for Biophysics, Saarland University, 66421 Homburg/Saar, Germany*; orcid.org/0000-0001-6734-2732

Matthias Hannig − *Clinic of Operative Dentistry, Periodontology and Preventive Dentistry, Saarland University, 66421 Homburg/Saar, Germany*

Complete contact information is available at: https://pubs.acs.org/10.1021/acsbiomaterials.1c00925

Funding

This study has been funded by the German Research Foundation (DFG) within the framework of the collaborative research center CRC 1027 (projects B1, B2, B3), DFG-project 415956642, using scientific instruments granted under DFG project number 449375068. Karin Jacobs acknowleges funding by the Max Planck School "Matter to Life".

Notes

The authors declare no competing financial interest.

ACKNOWLEDGMENTS

The authors thank Philipp Jung, Simone Trautmann, Erik Maikranz, and Michael Klatt for their guidance and advice. Special thanks goes to Thomas Faidt for creating the table of contents graphic.

ABBREVIATIONS

PBS, phosphate buffered saline; AFM, atomic force microscope; XPS, X-ray photoelectron spectroscopy; OCA, optical contact angle; SD, surface delay; BP, blood plasma; HAp, hydroxyapatite

REFERENCES

(1) Roveri, N.; Iafisco, M. Evolving Application of Biomimetic Nanostructured Hydroxyapatite. *Nanotechnol., Sci. Appl.* **2010**, *3*, 107.

(2) Qamar, Z.; Haji Abdul Rahim, Z. B.; Chew, H. P.; Fatima, T. Influence of trace elements on dental enamel properties: A review. *J. Pak Med. Assoc.* **2017**, *67* (1), 116−120.

(3) Clarke, B. Normal bone anatomy and physiology. *Clin J. Am. Soc. Nephrol.* **2008**, *3*, S131−S139.

(4) Lahiri, D.; Ghosh, S.; Agarwal, A. Carbon Nanotube Reinforced Hydroxyapatite Composite for Orthopedic Application: A Review. *Mater. Sci. Eng., C* **2012**, *32* (7), 1727−1758.

(5) Teixeira, S.; Rodriguez, M. A.; Pena, P.; De Aza, A. H.; De Aza, S.; Ferraz, M. P.; Monteiro, F. J. Physical Characterization of Hydroxyapatite Porous Scaffolds for Tissue Engineering. *Mater. Sci. Eng., C* **2009**, *29* (5), 1510−1514.

(6) Sorrentino, R.; Cochis, A.; Azzimonti, B.; Caravaca, C.; Chevalier, J.; Kuntz, M.; Porporati, A. A.; Streicher, R. M.; Rimondini, L. Reduced Bacterial Adhesion on Ceramics Used for Arthroplasty Applications. *J. Eur. Ceram. Soc.* **2018**, *38* (3), 963−970.

(7) Niinomi, M. Mechanical Properties of Biomedical Titanium Alloys. *Mater. Sci. Eng., A* **1998**, *243* (1−2), 231−236.

(8) Brady, R. A.; Calhoun, J. H.; Leid, J. G.; Shirtliff, M. E. Infections of Orthopaedic Implants and Devices. In *Springer Series on Biofilms*; Springer Berlin Heidelberg: pp 15−55, DOI: 10.1007/978-3-540-68119-9_2.

(9) Zhao, B.; van der Mei, H. C.; Subbiahdoss, G.; de Vries, J.; Rustema-Abbing, M.; Kuijer, R.; Busscher, H. J.; Ren, Y. Soft Tissue Integration versus Early Biofilm Formation on Different Dental Implant Materials. *Dent. Mater.* **2014**, *30* (7), 716−727.

(10) Douglas, C. W. I.; Naylor, K.; Phansopa, C.; Frey, A. M.; Farmilo, T.; Stafford, G. P. Physiological Adaptations of Key Oral Bacteria. In *Advances in Bacterial Pathogen Biology*; Elsevier: 2014; pp 257−335, DOI: 10.1016/bs.ampbs.2014.08.005.

(11) Filoche, S.; Wong, L.; Sissons, C. H. Oral Biofilms: Emerging Concepts in Microbial Ecology. *J. Dent. Res.* **2010**, *89* (1), 8−18.

(12) Hogan, S.; Stevens, N. T.; Humphreys, H.; O'Gara, J. P.; O'Neill, E. Current and Future Approaches to the Prevention and Treatment of Staphylococcal Medical Device-Related Infections. *Curr. Pharm. Des.* **2014**, *21* (1), 100−113.

(13) Camps-Font, O.; Figueiredo, R.; Valmaseda-Castellón, E.; Gay-Escoda, C. Postoperative Infections After Dental Implant Placement. *Implant Dent.* **2015**, *24*, 713.

(14) Campoccia, D.; Montanaro, L.; Arciola, C. R. A Review of the Biomaterials Technologies for Infection-Resistant Surfaces. *Biomaterials* **2013**, *34* (34), 8533−8554.

(15) Donlan, R. M.; Costerton, J. W. Biofilms: Survival Mechanisms of Clinically Relevant Microorganisms. *Clin. Microbiol. Rev.* **2002**, *15* (2), 167−193.

(16) Lebeaux, D.; Ghigo, J.-M.; Beloin, C. Biofilm-Related Infections: Bridging the Gap between Clinical Management and Fundamental Aspects of Recalcitrance toward Antibiotics. *Microbiol. Mol. Biol. Rev.* **2014**, *78* (3), 510−543.

(17) Mathelié-Guinlet, M.; Viela, F.; Viljoen, A.; Dehullu, J.; Dufrêne, Y. F. Single-Molecule Atomic Force Microscopy Studies of Microbial Pathogens. *Curr. Opin. Biomed. Eng.* **2019**, *12*, 1−7.

(18) Schmitt, Y.; Hähl, H.; Gilow, C.; Mantz, H.; Jacobs, K.; Leidinger, O.; Bellion, M.; Santen, L. Structural Evolution of Protein-Biofilms: Simulations and Experiments. *Biomicrofluidics* **2010**, *4* (3), 032201.
(19) van der Mei, H. C.; Rustema-Abbing, M.; de Vries, J.; Busscher, H. J. Bond Strengthening in Oral Bacterial Adhesion to Salivary Conditioning Films. *Appl. Environ. Microbiol.* **2008**, *74* (17), 5511−5515.
(20) *Handbook of Bacterial Adhesion: Principles, Methods, and Applications*, 1st ed.; An, Y. H., Friedman, R. J., Eds.; Humana Press: New York, NY, 2000; DOI: 10.1007/978-1-59259-224-1.
(21) Bouxsein, M. L.; Myburgh, K. H.; van der Meulen, M. C. H.; Lindenberger, E.; Marcus, R. Age-Related Differences in Cross-Sectional Geometry of the Forearm Bones in Healthy Women. *Calcif. Tissue Int.* **1994**, *54* (2), 113−118.
(22) Clemens, J. A. M.; Klein, C. P. A. T.; Vriesde, R. C.; Rozing, P. M.; de Groot, K. Healing of Large (2 Mm) Gaps around Calcium Phosphate-Coated Bone Implants: A Study in Goats with a Follow-up of 6 Months. *J. Biomed. Mater. Res.* **1998**, *40* (3), 341−349.
(23) Bigi, A.; Boanini, E.; Bracci, B.; Facchini, A.; Panzavolta, S.; Segatti, F.; Sturba, L. Nanocrystalline Hydroxyapatite Coatings on Titanium: A New Fast Biomimetic Method. *Biomaterials* **2005**, *26* (19), 4085−4089.
(24) Bhardwaj, G.; Yazici, H.; Webster, T. J. Reducing Bacteria and Macrophage Density on Nanophase Hydroxyapatite Coated onto Titanium Surfaces without Releasing Pharmaceutical Agents. *Nanoscale* **2015**, *7* (18), 8416−8427.
(25) Eliaz, N.; Ritman-Hertz, O.; Aronov, D.; Weinberg, E.; Shenhar, Y.; Rosenman, G.; Weinreb, M.; Ron, E. The Effect of Surface Treatments on the Adhesion of Electrochemically Deposited Hydroxyapatite Coating to Titanium and on Its Interaction with Cells and Bacteria. *J. Mater. Sci.: Mater. Med.* **2011**, *22* (7), 1741−1752.
(26) Valotteau, C.; Prystopiuk, V.; Pietrocola, G.; Rindi, S.; Peterle, D.; De Filippis, V.; Foster, T. J.; Speziale, P.; Dufrêne, Y. F. Single-Cell and Single-Molecule Analysis Unravels the Multifunctionality of The Staphylococcus Aureus Collagen-Binding Protein Cna. *ACS Nano* **2017**, *11* (2), 2160−2170.
(27) El-Kirat-Chatel, S.; Beaussart, A. Probing Bacterial Adhesion at the Single-Molecule and Single-Cell Levels by AFM-Based Force Spectroscopy. In *Nanoscale Imaging*; Methods in Molecular Biology; Springer: New York, 2018; pp 403−414, DOI: 10.1007/978-1-4939-8591-3_24.
(28) Zuttion, F.; Ligeour, C.; Vidal, O.; Wälte, M.; Morvan, F.; Vidal, S.; Vasseur, J.-J.; Chevolot, Y.; Phaner-Goutorbe, M.; Schillers, H. The Anti-Adhesive Effect of Glycoclusters OnPseudomonas Aeruginosa-bacteria Adhesion to Epithelial Cells Studied by AFM Single Cell Force Spectroscopy. *Nanoscale* **2018**, *10* (26), 12771−12778.
(29) Römling, U.; Balsalobre, C. Biofilm Infections, Their Resilience to Therapy and Innovative Treatment Strategies. *J. Int. Med.* **2012**, *272* (6), 541−561.
(30) Smith, A. J.; Robertson, D.; Tang, M. K.; Jackson, M. S.; MacKenzie, D.; Bagg, J. Staphylococcus Aureus in the Oral Cavity: A Three-Year Retrospective Analysis of Clinical Laboratory Data. *Br. Dent. J.* **2003**, *195* (12), 701−703.
(31) Merghni, A.; Bekir, K.; Kadmi, Y.; Dallel, I.; Janel, S.; Bovio, S.; Barois, N.; Lafont, F.; Mastouri, M. Adhesiveness of Opportunistic Staphylococcus Aureus to Materials Used in Dental Office: In Vitro Study. *Microb. Pathog.* **2017**, *103*, 129−134.
(32) Lee, A.; Wang, H.-L. Biofilm Related to Dental Implants. *Implant Dent.* **2010**, *19* (5), 387−393.
(33) Lorenzetti, M.; Dogša, I.; Stošicki, T.; Stopar, D.; Kalin, M.; Kobe, S.; Novak, S. The Influence of Surface Modification on Bacterial Adhesion to Titanium-Based Substrates. *ACS Appl. Mater. Interfaces* **2015**, *7* (3), 1644−1651.
(34) Maikranz, E.; Spengler, C.; Thewes, N.; Thewes, A.; Nolle, F.; Jung, P.; Bischoff, M.; Santen, L.; Jacobs, K. Different Binding Mechanisms of Staphylococcus Aureus to Hydrophobic and Hydrophilic Surfaces. *Nanoscale* **2020**, *12* (37), 19267−19275.
(35) Nilebäck, L.; Widhe, M.; Seijsing, J.; Bysell, H.; Sharma, P. K.; Hedhammar, M. Bioactive Silk Coatings Reduce the Adhesion of Staphylococcus Aureus While Supporting Growth of Osteoblast-like Cells. *ACS Appl. Mater. Interfaces* **2019**, *11* (28), 24999−25007.
(36) Kumari, S.; Lang, G.; DeSimone, E.; Spengler, C.; Trossmann, V. T.; Lücker, S.; Hudel, M.; Jacobs, K.; Krämer, N.; Scheibel, T. Engineered Spider Silk-Based 2D and 3D Materials Prevent Microbial Infestation. *Mater. Today* **2020**, *41*, 21.
(37) Goldmann, D. A.; Pier, G. B. Pathogenesis of Infections Related to Intravascular Catheterization. *Clin. Microbiol. Rev.* **1993**, *6* (2), 176−192.
(38) Gunaratnam, G.; Spengler, C.; Trautmann, S.; Jung, P.; Mischo, J.; Wieland, B.; Metz, C.; Becker, S.; Hannig, M.; Jacobs, K.; Bischoff, M. Human blood plasma factors affect the adhesion kinetics of Staphylococcus aureus to central venous catheters. *Sci. Rep.* **2020**, DOI: 10.1038/s41598-020-77168-x.
(39) Bowen, W. H.; Burne, R. A.; Wu, H.; Koo, H. Oral Biofilms: Pathogens, Matrix, and Polymicrobial Interactions in Microenvironments. *Trends Microbiol.* **2018**, *26* (3), 229−242.
(40) Spengler, C.; Thewes, N.; Nolle, F.; Faidt, T.; Umanskaya, N.; Hannig, M.; Bischoff, M.; Jacobs, K. Enhanced Adhesion Of Streptococcus Mutans to Hydroxyapatite after Exposure to Saliva. *J. Mol. Recognit.* **2017**, *30* (7), e2615.
(41) Hannig, M.; Joiner, A. The Structure, Function and Properties of the Acquired Pellicle. In *Monographs in Oral Science*; Karger: 2006; pp 29−64, DOI: 10.1159/000090585.
(42) Güth-Thiel, S.; Kraus-Kuleszka, I.; Mantz, H.; Hoth-Hannig, W.; Hähl, H.; Dudek, J.; Jacobs, K.; Hannig, M. Comprehensive Measurements of Salivary Pellicle Thickness Formed at Different Intraoral Sites on Si Wafers and Bovine Enamel. *Colloids Surf., B* **2019**, *174*, 246−251.
(43) Trautmann, S.; Künzel, N.; Fecher-Trost, C.; Barghash, A.; Schalkowsky, P.; Dudek, J.; Delius, J.; Helms, V.; Hannig, M. Deep Proteomic Insights into the Individual Short-Term Pellicle Formation on Enamel - An In Situ Pilot Study. *Proteomics: Clin. Appl.* **2020**, *14* (3), 1900090.
(44) Thewes, N.; Loskill, P.; Spengler, C.; Hümbert, S.; Bischoff, M.; Jacobs, K. A Detailed Guideline for the Fabrication of Single Bacterial Probes Used for Atomic Force Spectroscopy. *Eur. Phys. J. E* **2015**, *38* (12), 140 DOI: 10.1140/epje/i2015-15140-2.
(45) Zeitz, C.; Faidt, T.; Grandthyll, S.; Hähl, H.; Thewes, N.; Spengler, C.; Schmauch, J.; Deckarm, M. J.; Gachot, C.; Natter, H.; Hannig, M.; Müller, F.; Jacobs, K. Synthesis of Hydroxyapatite Substrates: Bridging the Gap between Model Surfaces and Enamel. *ACS Appl. Mater. Interfaces* **2016**, *8* (39), 25848−25855.
(46) Nakamichi, I.; Iwaku, M.; Fusayama, T. Bovine teeth as possible substitutes in the adhesion test. *J. Dent Res.* **1983**, *62* (10), 1076.
(47) Laurance-Young, P.; Bozec, L.; Gracia, L.; Rees, G.; Lippert, F.; Lynch, R. J. M.; Knowles, J. C. A review of the structure of human and bovine dental hard tissues and their physicochemical behaviour in relation to erosive challenge and remineralisation. *J. Dent.* **2011**, *39* (4), 266.
(48) Arango-Santander, S.; Montoya, C.; Pelaez-Vargas, A.; Ossa, E. A. Chemical, structural and mechanical characterization of bovine enamel. *Arch Oral Biol.* **2020**, *109*, 104573.
(49) Ayoub, H. M.; Gregory, R. L.; Tang, Q.; Lippert, F. Comparison of human and bovine enamel in a microbial caries model at different biofilm maturations. *Journal of Dentistry* **2020**, *96*.
(50) Shirley, D. A. High-Resolution X-Ray Photoemission Spectrum of the Valence Bands of Gold. *Phys. Rev. B* **1972**, *5* (12), 4709−4714.
(51) Yeh, J. J.; Lindau, I. Atomic Subshell Photoionization Cross Sections and Asymmetry Parameters: $1 \leqslant Z \leqslant 103$. *At. Data Nucl. Data Tables* **1985**, *32* (1), 1−155.
(52) Beaussart, A.; El-Kirat-Chatel, S.; Herman, P.; Alsteens, D.; Mahillon, J.; Hols, P.; Dufrêne, Y. F. Single-Cell Force Spectroscopy of Probiotic Bacteria. *Biophys. J.* **2013**, *104* (9), 1886−1892.
(53) Aguayo, S.; Donos, N.; Spratt, D.; Bozec, L. Nanoadhesion of Staphylococcus Aureus onto Titanium Implant Surfaces. *J. Dent. Res.* **2015**, *94* (8), 1078−1084.
(54) Dufrêne, Y. F. Sticky Microbes: Forces in Microbial Cell Adhesion. *Trends Microbiol.* **2015**, *23* (6), 376−382.

(55) Cohen, J. Statistical Power Analysis. *Curr. Dir. Psychol. Sci.* **1992**, *1* (3), 98−101.
(56) Han, Y. Effects of brief sodium fluoride treatments on the growth of early and mature cariogenic biofilms. *Sci. Rep.* **2021**, *11* (1), 18290.
(57) Walsh, T.; Worthington, H. V.; Glenny, A.-M.; Marinho, V. C.; Jeroncic, A. Fluoride Toothpastes of Different Concentrations for Preventing Dental Caries. *Cochrane Database of Syst. Rev.* **2019**, DOI: 10.1002/14651858.CD007868.pub3.
(58) Featherstone, J. D. B. Prevention and Reversal of Dental Caries: Role of Low Level Fluoride. *Community Dent. and Oral Epidemiol.* **1999**, *27*, 31−40.
(59) Kirsch, J.; Hannig, M.; Winkel, P.; Basche, S.; Leis, B.; Pütz, N.; Kensche, A.; Hannig, C. Influence of pure fluorides and stannous ions on the initial bacterial colonization in situ. *Sci. Rep.* **2019**, *9* (1), 18499.
(60) Loskill, P.; Zeitz, C.; Grandthyll, S.; Thewes, N.; Müller, F.; Bischoff, M.; Herrmann, M.; Jacobs, K. Reduced adhesion of oral bacteria on hydroxyapatite by fluoride treatment. *Langmuir.* **2013**, *29* (18), 5528−33.
(61) Dorobantu, L. S.; Bhattacharjee, S.; Foght, J. M.; Gray, M. R. Atomic Force Microscopy Measurement of Heterogeneity in Bacterial Surface Hydrophobicity. *Langmuir* **2008**, *24* (9), 4944−4951.
(62) Vissers, T.; Brown, A. T.; Koumakis, N.; Dawson, A.; Hermes, M.; Schwarz-Linek, J.; Schofield, A. B.; French, J. M.; Koutsos, V.; Arlt, J.; Martinez, V. A.; Poon, W. C. K. Bacteria as Living Patchy Colloids: Phenotypic Heterogeneity in Surface Adhesion. *Sci. Adv.* **2018**, *4* (4), eaao1170.
(63) Bevilacqua, L.; Milan, A.; Del Lupo, V.; Maglione, M.; Dolzani, L. Biofilms Developed on Dental Implant Titanium Surfaces with Different Roughness: Comparison Between In Vitro and In Vivo Studies. *Curr. Microbiol.* **2018**, *75* (6), 766−772.
(64) Wang, C.; Zhao, Y.; Zheng, S.; Xue, J.; Zhou, J.; Tang, Y.; Jiang, L.; Li, W. Effect of Enamel Morphology on Nanoscale Adhesion Forces of Streptococcal Bacteria : An AFM Study. *Scanning* **2015**, *37* (5), 313−321.
(65) Davoudi, N.; Huttenlochner, K.; Chodorski, J.; Schlegel, C.; Bohley, M.; Müller-Renno, C.; Aurich; Jan, C.; Ulber, R.; Ziegler, C. Adhesion Forces of the Sea-Water Bacterium Paracoccus Seriniphilus on Titanium: Influence of Microstructures and Environmental Conditions. *Biointerphases* **2017**, *12* (5), 05G606.
(66) Spengler, C.; Nolle, F.; Mischo, J.; Faidt, T.; Grandthyll, S.; Thewes, N.; Koch, M.; Müller, F.; Bischoff, M.; Klatt, M. A.; Jacobs, K. Strength of Bacterial Adhesion on Nanostructured Surfaces Quantified by Substrate Morphometry. *Nanoscale* **2019**, *11* (42), 19713−19722.
(67) Spengler, C.; Thewes, N.; Jung, P.; Bischoff, M.; Jacobs, K. Determination of the Nano-Scaled Contact Area of Staphylococcal Cells. *Nanoscale* **2017**, *9* (28), 10084−10093.
(68) Sarshar, M. A.; Xu, W.; Choi, C.-H. Correlation between Contact Line Pinning and Contact Angle Hysteresis on Heterogeneous Surfaces: A Review and Discussion. In *Advances in Contact Angle, Wettability and Adhesion*; John Wiley & Sons, Inc.: 2013; pp 1−18, DOI: 10.1002/9781118795620.ch1.
(69) de Gennes, P. G. (1985). "Wetting: Statics and dynamics,. *Rev. Mod. Phys.* **1985**, *57*, 827−863.
(70) Legeay, G.; Poncin-Epaillard, F.; Arciola, C. R. New Surfaces with Hydrophilic/Hydrophobic Characteristics in Relation to (No)-Bioadhesion. *Int. J. Artif. Organs* **2006**, *29* (4), 453−461.
(71) Tang, P.; Zhang, W.; Wang, Y.; Zhang, B.; Wang, H.; Lin, C.; Zhang, L. Effect of Superhydrophobic Surface of Titanium On Staphylococcus Aureus Adhesion. *J. Nanomater.* **2011**, *2011*, 1−8.
(72) Boks, N. P.; Busscher, H. J.; van der Mei, H. C.; Norde, W. Bond-Strengthening in Staphylococcal Adhesion to Hydrophilic and Hydrophobic Surfaces Using Atomic Force Microscopy. *Langmuir* **2008**, *24* (22), 12990−12994.
(73) Spengler, C.; Glatz, B. A.; Maikranz, E.; Bischoff, M.; Klatt, M. A.; Santen, L.; Fery, A.; Jacobs, K. The Adhesion Capability of S. Aureus Cells Is Heterogeneously Distributed over the Cell Envelope. *bioRxiv* **2021**, DOI: 10.1101/2021.01.05.425282.
(74) van der Westen, R.; Sjollema, J.; Molenaar, R.; Sharma, P. K.; van der Mei, H. C.; Busscher, H. J. Floating and Tether-Coupled Adhesion of Bacteria to Hydrophobic and Hydrophilic Surfaces. *Langmuir* **2018**, *34* (17), 4937−4944.
(75) Sjollema, J.; van der Mei, H. C.; Hall, C. L.; Peterson, B. W.; de Vries, J.; Song, L.; Jong, E. D. de; Busscher, H. J.; Swartjes, J. J. T. M. Detachment and successive re-attachment of multiple, reversibly-binding tethers result in irreversible bacterial adhesion to surfaces. *Sci. Rep* **2017**, *7*, 4369.
(76) Clarke, S. R.; Foster, S. J. Surface Adhesins of Staphylococcus Aureus. In *Advances in Microbial Physiology*; Elsevier: 2006; Vol. *51*, pp 187−224, DOI: 10.1016/S0065-2911(06)51004-5.
(77) Xu, C.-P.; van de Belt-Gritter, B.; Dijkstra, R. J. B.; Norde, W.; van der Mei, H. C.; Busscher, H. J. Interaction Forces between Salivary Proteins And Streptococcus Mutans with and without Antigen I/II. *Langmuir* **2007**, *23* (18), 9423−9428.
(78) Bridgett, M. J.; Davies, M. C.; Denyer, S. P. Control of Staphylococcal Adhesion to Polystyrene Surfaces by Polymer Surface Modification with Surfactants. *Biomaterials* **1992**, *13* (7), 411−416.
(79) Patel, J. D.; Ebert, M.; Ward, R.; Anderson, J. M. S. Epidermidis Biofilm Formation: Effects of Biomaterial Surface Chemistry and Serum Proteins. *J. Biomed. Mater. Res.* **2007**, *80A* (3), 742−751.
(80) Faidt, T.; Friedrichs, A.; Grandthyll, S.; Spengler, C.; Jacobs, K.; Müller, F. Effect of Fluoride Treatment on the Acid Resistance of Hydroxyapatite. *Langmuir* **2018**, *34* (50), 15253−15258.
(81) Faidt, T.; Zeitz, C.; Grandthyll, S.; Hans, M.; Hannig, M.; Jacobs, K.; Müller, F. Time Dependence of Fluoride Uptake in Hydroxyapatite. *ACS Biomater. Sci. Eng.* **2017**, *3* (8), 1822−1826.
(82) Robinson, C.; Brookes, S. J.; Shore, R. C.; Kirkham, J. The Developing Enamel Matrix: Nature and Function. *Eur. J. Oral Sci.* **1998**, *106* (S1), 282−291.